Optics Communications 285 (2012) 5337–5340

Contents lists available at SciVerse ScienceDirect

Optics Communications

journal homepage: www.elsevier.com/locate/optcom

Reconstruction of surface profile by using heterodyne moiré method

Wei-Yao Chang [a], Fan-Hsi Hsu [a], Kun-Huang Chen [b,*], Jing-Heng Chen [c], Hung-Chih Hsieh [a], Ken Y. Hsu [a]

[a] Department of Photonics and Institute of Electro-Optical Engineering, National Chiao-Tung University, Hsinchu County 30050, Taiwan
[b] Department of Electrical Engineering, Feng Chia University, 100 Wenhwa Road, Seatwen, Taichung 40724, Taiwan
[c] Department of Photonics, Feng Chia University,100 Wenhwa Road, Seatwen, Taichung 40724, Taiwan

ARTICLE INFO

Article history:
Received 26 June 2012
Received in revised form
27 July 2012
Accepted 29 July 2012
Available online 10 August 2012

Keywords:
Surface profile measurement
Moiré
Heterodyne interferometry

ABSTRACT

Based on the projection moiré method and heterodyne interferometry, this study proposes an alternative method for reconstructing the surface profile of an object. Obliquely illuminating a linear grating with an expanding collimated light, a self-image of this grating can be generated and projected on the surface of the tested object. The grating fringes distorted by the surface profile are imaged on the reference grating to form the moiré fringes. These moiré fringes are then captured by a CMOS camera. If the projection grating moves with a constant velocity along the grating plane, each pixel of the CMOS camera records a series of sampling points of the sinusoidal wave. These sinusoidal waves behave like heterodyne interferometric signals. Hence, the accurate and stable phase distribution of the tested object surface can be obtained using the IEEE 1241 least-squares sine fitting algorithm and 2D phase unwrapping. Substituting the phase values into the derived equation, the surface profile of the tested object can be reconstructed. The experiments in this study verified the feasibility of this method, showing a measurement resolution of approximately 1.9 μm. The proposed measurement method has the merits of both the projection moiré method and the heterodyne interferometry.

1. Introduction

The technique of object surface profiling is widely applied in industrial and optical testing [1,2]. The requisitions for rapid, highly accurate, and high-resolution measurements have increased the demand for non-contact and real-time measurement methods. Common methods of object surface profiling include the optical edge projection method [3], the fringe projection method [4–6], the coded structured light projection method [7,8], and the moiré method [9–12]. The optical edge projection method is based on the geometric relationships between the shadows of the object edge and reference lines, and scans the entire surface of the test object to obtain object profiles. The drawback of this method is the complex edge contour algorithm and its low measurement resolution. The fringe projection method and the coded-structured light projection method feature simple structures and rapid, full-field measurement. But owing to the limited ability of directly analyzing the projection fringes, the measurement resolutions are much lower because of the influence by the pitch and the quality of the projection fringes and the resolution of the camera. The moiré method uses a shadow or a projection setup to generate moiré fringes for object profiling. Moiré fringes are formed by the geographic interference of the grating fringes and can be analyzed to reconstruct the surface profile. Lino and Dal Fabbro[13] further reconstructed the 3D surface profile by rotating tested object to capture moiré fringes under multiple angles. Because these techniques do not directly analyze the projection fringes, they have much higher measurement sensitivity and resolution than the above mentioned method. However, the resolution of this approach is relatively low because of the light source stability. Therefore, this study proposes an alternative method for measuring the object surface profile using the projection moiré method and heterodyne interferometry. Because it applies the projection moiré method, the proposed method can inspect the larger degrees of the surface flexibility, and the longitudinal and lateral range on the sample surface. Using heterodyne interferometry ensures that this method is simple to implement, highly accurate, and achieves high resolution. Experimental results confirm the feasibility of this measuring method, which has a measurement resolution of approximately 1.9 μm.

2. Principle

Fig. 1 shows the experimental setup for this measurement. For convenience, the $+z$-axis is set in the direction of light propagation, and the y-axis is set perpendicular to the plane of the paper. An expanding collimated light with a wavelength of λ incident onto a projection grating G_1 generates a first-order self-image on the surface of a tested object at a projection angle of α.

* Corresponding author. Tel.: +886 4 2451 7250; fax: +886 4 2451 6842.
E-mail address: chenkh@fcu.edu.tw (K.-H. Chen).

0030-4018/$ - see front matter © 2012 Elsevier B.V. All rights reserved.
http://dx.doi.org/10.1016/j.optcom.2012.07.079

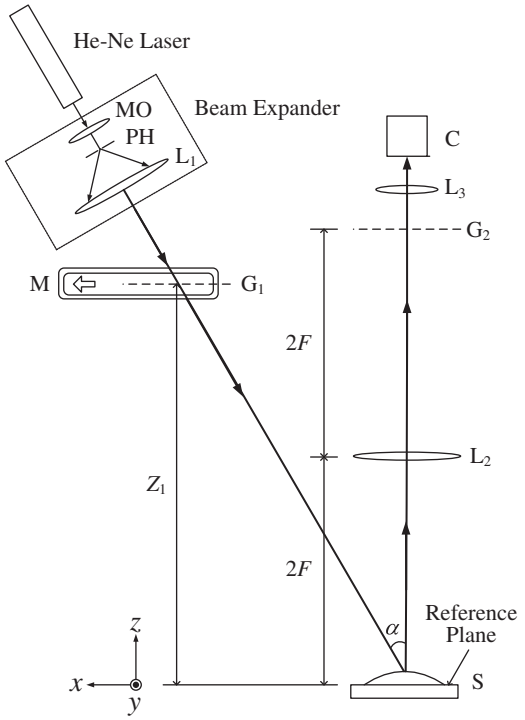

Fig. 1. Optical configuration.

The position of the first-order self-image can be expressed as [14]

$$Z_1 = \frac{p^2}{\lambda}\cos^3\alpha, \tag{1}$$

where p is the pitch of the grating G_1. The reflected grating fringes of the object's surface is projected on the reference grating G_2 with the same pitch p as an imaging lens L_2 with $1\times$ magnification. This forms moiré fringes, which can be captured by a CMOS camera C. When a motorized translation stage M moves the projection-grating G_1 along the grating plane at a constant velocity, each pixel of the CMOS camera records a series of sampling points of the sinusoidal wave. These sinusoidal waves behave like heterodyne interferometric signals. Hence, the light intensity at the CMOS camera C can be expressed as [12]

$$I(x,y) = I_0(x,y) + \gamma(x,y)\cos[\theta(x,y) + \varphi], \tag{2}$$

where $I_0(x, y)$ and $\gamma(x, y)$ are the average intensity and visibility of the signal, respectively, and φ is the phase difference caused by moving the grating G_1. This phase difference can be expressed as

$$\varphi = \frac{2\pi v t}{p} = 2\pi f t, \tag{3}$$

where f is the heterodyne frequency induced by the time-variable phase. Eq. (2) shows that $\theta(x, y)$ is the phase distribution of the object surface, which can be expressed as

$$\theta(x,y) = \frac{2\pi}{p}h(x,y)\tan\alpha. \tag{4}$$

where $h(x, y)$ is the height distribution of the object surface. Eq. (4) can be rewritten as

$$h(x,y) = \frac{p}{2\pi\tan\alpha}\theta(x,y) \tag{5}$$

Eq. (5) shows that the height distribution $h(x, y)$ of the object surface can be obtained by measuring the phase distribution $\theta(x, y)$. To obtain the value of $\theta(x, y)$, rewrite Eq. (2) as

$$\begin{aligned} I(x,y) &= I_0(x,y) + \gamma(x,y)\cos[2\pi f t + \theta(x,y)] \\ &= A\cos(2\pi f t) + B\sin(2\pi f t) + C, \end{aligned} \tag{6}$$

where A, B, and C are real numbers, and the relationship between A, B, and $\theta(x, y)$ can be shown as

$$\theta(x,y) = \tan^{-1}\left(\frac{-B}{A}\right) \tag{7}$$

Terms A and B can be estimated by the IEEE 1241 least-squares sine wave fitting algorithm [15]. Substituting A and B into Eq. (7) yields the corresponding phase $\theta(x, y)$ of the pixel. The phase distribution of the sample surface can be obtained by applying this procedure to the other pixels and using 2D phase unwrapping [16]. The surface profile of the tested object can then be reconstructed using Eq. (5).

3. Experimental setup

To show the validity of the proposed method, a diffusive convex object with a radius r of 25.4 mm and a central height h_c of 2.1 mm (Fig. 2) was profiled at 25 °C. The experimental setup consisted of a He–Ne laser with a wavelength of 632.8 nm, two linear gratings with a pitch of 0.5 mm, an imaging lens with a focal length of 200 mm, a motorized stage (Sigma Koki/SGSP(MS)26-100) with a resolution of 1 μm to generate a heterodyne frequency f of 10 Hz ($v = 5$ mm/s), and a CMOS camera (Basler/A504k) with an 8-bit gray level and a 1280×1024 image resolution. For convenience, the projection angle α was set to 30°. The frame rate f_s and the exposure time Δt of the CMOS camera were set to 150 fps and 6 ms, respectively. The total recording time t was 1 s to record the interference signal in a continuous time.

4. Results and discussions

Figs. 3 and 4 show the experimental results. Fig. 3a and b show the moiré patterns at 0 s and 7/150 s (phase difference 8/15 period). Fig. 3c and d show the results of filtering Fig. 3a and b using a 2D median filter with a 5×5 window. The least-squares sine wave fitting algorithm and 2D phase unwrapping can then obtain the phase distribution of the tested object surface with respect to the reference plane. After substituting the phase distribution into Eq. (5), it is possible to reconstruct the surface profile of the tested object (Fig. 4). Fig. 4 shows the surface profile and the height distribution of the diffusive convex object. The black dots in Fig. 5 correspond to the red segment in Fig. 4, and the solid line is the simulated curve of the convex object. These experimental results correspond well with the simulated curve.

The moiré patterns in Fig. 3 show the bright spots at the left side. These spots are from the reflected light beam of the object surface, which is immediately along the observation axis (z-axis). Thus, the camera records considerably more light intensity in this region. Because the proposed method has the same property of the heterodyne interferometry, the measured phase can be affected less by the stability of the light source and the non-uniformity of the light intensity on the sample surface. Therefore, the surface profile can still be reconstructed, as the experimental results shown.

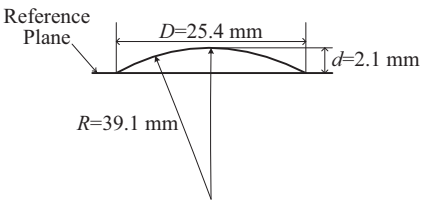

Fig. 2. Specification of tested sample.

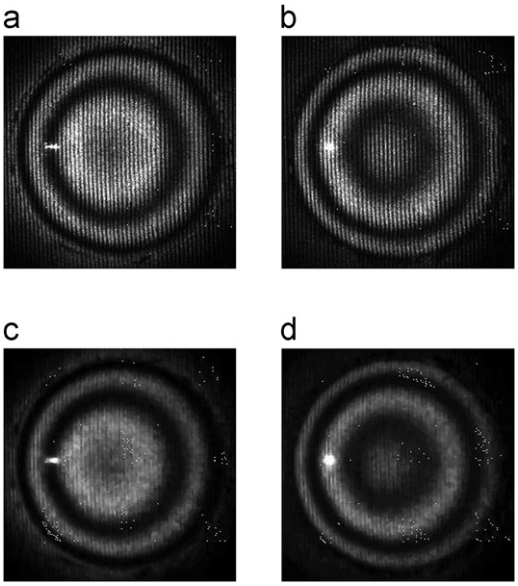

Fig. 3. Moiré patterns recorded by CMOS camera. Fig. 3a and b show the moiré patterns at 0 s and 7/150 s (phase difference 8/15 period). Fig. 3c and d show the results of filtering Fig. 3a and b.

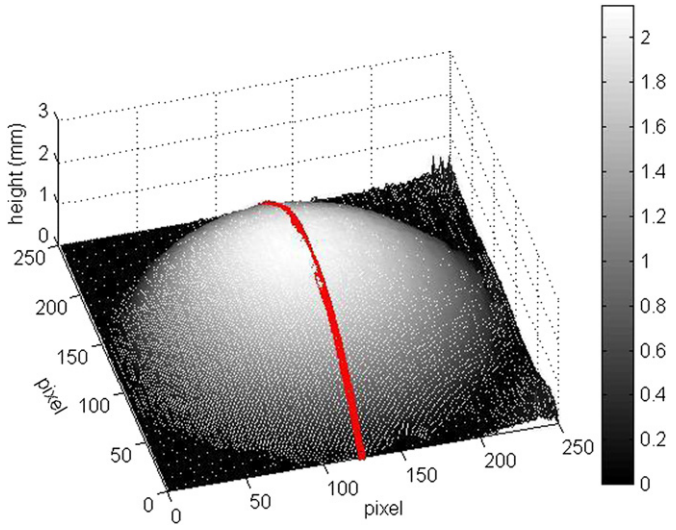

Fig. 4. The surface profile and the height distribution of the diffusive convex object. Where red line is a cross section line of the sample surface which is drawing along the 123th pixel of the *x*-direction. (For interpretation of the references to color in this figure legend, the reader is referred to the web version of this article.)

According to Eq. (5), the height error Δh of this method can be expressed as

$$\Delta h = \left|\frac{\partial h}{\partial p}\Delta p\right| + \left|\frac{\partial h}{\partial \alpha}\Delta \alpha\right| + \left|\frac{\partial h}{\partial \theta}\Delta \theta\right|, \tag{8}$$

where Δp, $\Delta \alpha$, and $\Delta \theta$ denote the grating pitch error, the projection angle error, and the phase error. The grating pitch error Δp caused by the grating fabrication is approximately 6.7×10^{-5} mm. Considering the axis alignment error, and the resolution of the rotational stage, the projection angle error $\Delta \alpha$ is approximately 0.11°. The sampling error introduces the phase error $\Delta \theta$. Because the visibility of the moiré fringes in this experiment is 0.4, $\Delta \theta$ can be estimated to be 0.07° [17]. Substituting these values, the related experimental data, and the measurement results into Eq. (8) shows that the estimated height error is approximately 1.9 μm.

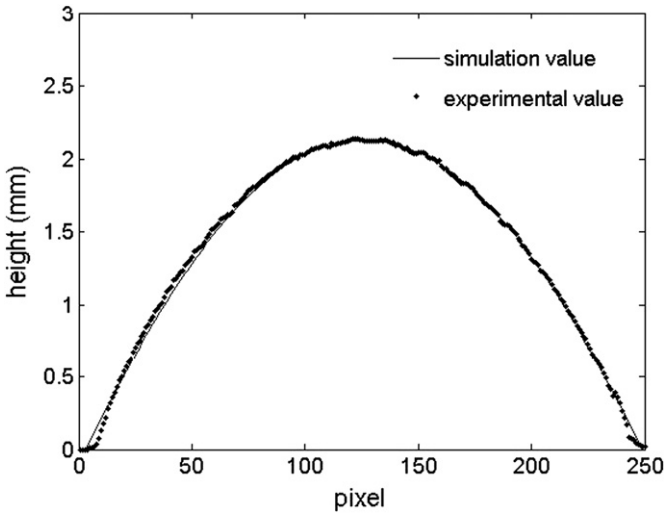

Fig. 5. Comparison figure of cross section line. The black dots correspond to the red segment in Fig. 4, and the solid line is the simulated curve of the convex object.

Eq. (5) can present one period of the moiré fringes, which corresponds to the height deviation of 0.866 mm, under the experimental condition of a $p=0.5$ mm and $\alpha=30°$ projection angle. Therefore, if the tested sample height is 2.1 mm, two periods of the moiré fringes can be presented (Fig. 3). Although setting more than one period of the moiré fringes can increase the measurement resolution, the resolution cannot increase infinitely. This is because a decrease in the grating pitch can increase the number of moiré fringes on the sample surface, but the limited pixel size of the camera limits the ability of analyzing the periodic intensity variation of the moiré fringes. Therefore, the values of the grating pitch and the projection angle adopted in the experiments in this study are appropriate settings for these conditions.

5. Conclusions

This study proposes an object surface profiling technique that uses the projection moiré method and heterodyne interferometry. To show the validity of the proposed method, a diffusive convex object was measured in the experiment. Results show a good correspondence with the simulated value, which is from the specification of the sample. The measurement resolution is approximately 1.9 μm. Thus, the proposed method offers the benefits of the projection moiré method and the heterodyne interferometry while retaining the merits of high stability and high resolution.

Acknowledgments

The authors would like to thank the National Science Council of the Republic of China, Taiwan for financially supporting this research under Contract nos. NSC 98-2221-E-009-018-MY3 and NSC 100-2221-E-035-062.

References

[1] W.V. Paepegema, A. Shulev, A. Moentjens, J. Harizanova, J. Degrieck, V. Sainov, Optics and Lasers in Engineering 46 (2008) 527.
[2] T. Nakazawa, J. Sasian, Optical Engineering 50 (2011) 053603.
[3] H. Miao, C. Quan, C.J. Tay, Y. Fu, X.P. Wu, Optics Communications 256 (2005) 16.
[4] C.J. Tay, M. Thakur, C. Quan, Applied Optics 44 (2005) 1393.

[5] C. Quan, X.Y. He, C.F. Wang, C.J. Tay, H.M. Shang, Optics Communications 189 (2001) 21.
[6] L. Huang, Q. Kemao, B. Pan, A.K. Asundi, Optics and Lasers in Engineering 48 (2010) 141.
[7] W.H. Su, Optics Express 15 (2007) 13167.
[8] E.H. Kim, J. Hahn, H. Kim, B. Lee, Optics Express 17 (2009) 7818.
[9] L. Jin, Y. Kodera, T. Yoshizawa, Y. Otani, Optical Engineering 39 (2000) 2119.
[10] J. Degrieck, W.V. Paepegem, P. Boone, Optics and Lasers in Engineering 36 (2001) 29.
[11] Y.B. Choi, S.W. Kim, Optical Engineering 37 (1998) 1005.
[12] S. Mirza, C. Shakher, Optical Engineering 44 (2005) 013601.
[13] A.C.L. Lino, I.M. Dal Fabbro, AIP Conference Proceedings 992 (2008) 1034.
[14] M. Testorfa, J. Jahnsa, N.A. Khilob, A.M. Goncharenkob, Optics Communications 129 (1996) 167.
[15] Y.L. Chen, Z.C. Jian, H.C. Hsieh, W.T. Wu, D.C. Su, Optical Engineering 47 (2008) 125601.
[16] K. Itoh, Applied Optics 21 (1982) 2470.
[17] H.C. Hsieh, W.T. Wu, W.Y. Chang, Y.L. Chen, D.C. Su, Optical Engineering 50 (2011) 045601.